

PROCEEDINGS OF SPIE

SPIDigitalLibrary.org/conference-proceedings-of-spie

Extensive study of the linewidth enhancement factor of a distributed feedback quantum cascade laser at ultra-low temperature

O. Spitz, A. Herdt, J. Duan, M. Carras, W. Elsässer, et al.

O. Spitz, A. Herdt, J. Duan, M. Carras, W. Elsässer, F. Grillot, "Extensive study of the linewidth enhancement factor of a distributed feedback quantum cascade laser at ultra-low temperature," Proc. SPIE 10926, Quantum Sensing and Nano Electronics and Photonics XVI, 1092619 (21 February 2019); doi: 10.1117/12.2510502

SPIE.

Event: SPIE OPTO, 2019, San Francisco, California, United States

Extensive study of the linewidth enhancement factor of a distributed feedback quantum cascade laser at ultra-low temperature

O. Spitz^{a,b}, A. Herdt^c, J. Duan^a, M. Carras^b, W. Elsässer^c, and F. Grillot^{a,d}

^aLTCI, Télécom ParisTech, Université Paris-Saclay, 46 rue Barrault, Paris, France

^bmirSense, Centre d'intégration NanoInnov, 8 avenue de la Vauve, Palaiseau, France

^cTechnische Universität Darmstadt, Schlossgartenstraße 7, D-64289 Darmstadt, Germany

^dCenter for High Technology Materials, University of New-Mexico, Albuquerque, NM USA

ABSTRACT

Quantum cascade lasers (QCLs) are optical sources exploiting radiative intersubband transitions within the conduction band of semiconductor heterostructures.¹ The opportunity given by the broad span of wavelengths that QCLs can achieve, from mid-infrared to terahertz, leads to a wide number of applications such as absorption spectroscopy, optical countermeasures and free-space communications requiring stable single-mode operation with a narrow linewidth and high output power.² One of the parameters of paramount importance for studying the high-speed and nonlinear dynamical properties of QCLs is the linewidth enhancement factor (LEF). The LEF quantifies the coupling between the gain and the refractive index of the QCL or, in a similar manner, the coupling between the phase and the amplitude of the electrical field.³ Prior work focused on experimental studies of the LEF for pump currents above threshold but without exceeding 12% of the threshold current at 283K⁴ and 56% of the threshold current at 82K.⁵ In this work, we use the Hakki-Paoli method⁶ to retrieve the LEF for current biases below threshold. We complement our findings using the self-mixing interferometry technique⁵ to obtain LEFs for current biases up to more than 100% of the threshold current. These insets are meaningful to understand the behavior of QCLs, which exhibit a strongly temperature sensitive chaotic bubble when subject to external optical feedback.⁷

Keywords: Quantum cascade lasers, Mid-infrared photonics, Linewidth enhancement factor, Alpha factor

1. INTRODUCTION

Quantum cascade lasers have been proven to be sensitive to external perturbations such as external optical feedback and injection and to display non-linear phenomena.⁷ Depending on the amount of external optical feedback and the length of the external cavity, the QCLs can enter five different non-linear regimes such as coherence collapse followed by restabilization for strong enough feedback ratios,⁸ similarly to what has been unveiled more than 30 years ago in the case of distributed feedback laser diodes.⁹ In interband lasers, the dynamical properties of the device are governed by several parameters of the lasers such as the carrier-to-photon lifetime,¹⁰ the differential gain of the materials¹¹ and the linewidth enhancement factor (LEF).¹² In this paper, we focus on the influence of the latter and study its evolution when varying the pump current. The LEF can also be found in the literature under the designation linewidth broadening factor or α -factor, since it is responsible for the linewidth broadening in the optical domain, resulting in a linewidth enhanced by a factor $(1 + \alpha^2)$ compared to the Shawlow-Townes limit. In laser diodes, experiments with several techniques, such as direct measurement of the subthreshold optical spectrum as the injected current is varied,¹³ radio-frequency measurements,¹⁴ analysis of the locking regimes induced by optical injection from a master laser,¹⁵ or optical feedback self-mixing effects,¹⁶ have proved that the LEF can vary between 1 and 8. This is known to be caused by the symmetry breaking in the two bands involved in the laser transition, resulting in a spectrally asymmetric differential gain. In contrast, both laser subbands of a QCL are within the conduction band, and exhibit the same reciprocal space curvature.¹⁷ This should lead to a zero LEF because of a symmetric differential gain. However, experimental works in the terahertz¹⁸ and the mid-infrared domain,¹⁹ showed that QCLs may exhibit a non-zero LEF.

Further author information: (Send correspondence to O.S.)

O.S.: E-mail: olivier.spitz@telecom-paristech.fr

2. DEVICE DESCRIPTION AND EXPERIMENTAL APPARATUS

The QCL under study is identical to the one presented in Ref. 10. It emits single mode at $5.45 \mu\text{m}$ under continuous bias at 77 K and it emits single mode at $5.63 \mu\text{m}$ under a 3% duty cycle at 290 K. The threshold of this laser is 331 mA at 77 K and 590 mA at 290 K. Below threshold this QCL behaves like a Fabry-Perot laser, as can be seen in Fig. 1 a). The epi-side down configuration of this QCL allows a continuous pumping for temperatures up to 150 K. The laser is inserted inside a cryostat with a ZnSe window with very high transmission at mid-infrared wavelength. The cryostat has a tank to be filled with liquid nitrogen when experiments are carried at 77 K. The exact temperature of the inside mount is given by a calibrated thermistance. A golden plated mirror is placed at 20 cm from the emitting facet of the QCL in the case of the self-mixing method. This mirror is periodically translated with a piezo controller. In the case of self-mixing interferometry, the feedback must be in the order of 10^{-6} at maximum²⁰ because otherwise, the self-mixing pattern is combined with non-linear dynamics such as oscillations and low frequency fluctuations (LFF).¹¹ A beam splitter with high reflection and low transmission is inserted between the feedback mirror and the QCL. The reflected light is analyzed through either a Mercury-Cadmium-Telluride (MCT) detector with a bandwidth of 50 MHz (Kolmar KMPV50 0.5 J2) for self-mixing interferometry or a Fourier transform infrared spectrometer (Bruker Vertex 80V) for the Hakki-Paoli method (and in that case, the feedback mirror is hidden). The low transmission of the plate allows achieving both weak feedback ratios for the self-mixing interferometry and high power for accurate detection and analysis. The MCT detector is linked to a fast oscilloscope (Tektronix TDS 6154 C) with a bandwidth of 40 GS/s for real time acquisition and analysis. The QCL is pumped continuously with a high precision current source (ILX Lightwave LDM-3232), from below threshold (minimum value of 255 mA) to 2.33 times the threshold current (maximum value of 770 mA).

3. MODELLING

Quantum cascade lasers are promising optical sources for secure communications since they emit in the mid-infrared domain. The latter is composed of two transparency windows, namely around $4 \mu\text{m}$ and around $10 \mu\text{m}$, and the high transmission of the atmosphere at these wavelengths²¹ paves the way for free-space communications, contrary to usual laser diodes used in telecommunication systems which require specific fibers. Secure communication can be achieved through the synchronization of a chaotic master laser with a slave laser. The message is subsequently hidden in the chaotic pattern of the master laser and then retrieved by subtracting the detector signal and the slave laser signal.²² The LEF has a major impact on the synchronization of the chaos because

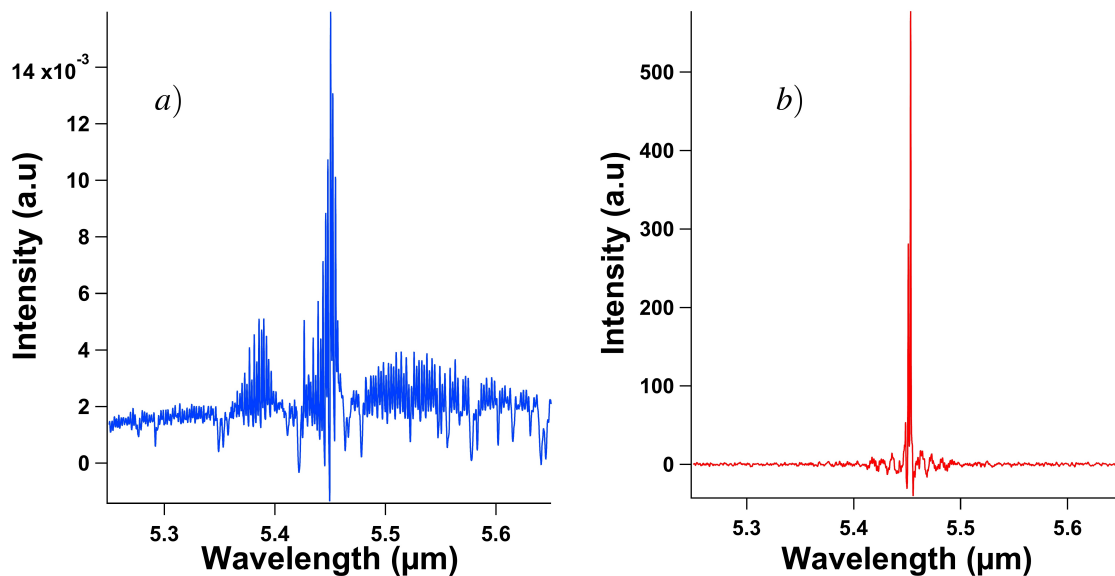


Figure 1: Spectral characteristics of the free-running QCL operating at 77 K and under a continuous bias just below threshold at 325 mA (a) and above threshold at 340 mA (b).

the master and the slave laser must be similar in order to allow the synchronization, except if the injection rate is large enough to access the amplification area.²³ Two lasers with similar characteristics in terms of wavelength or photon lifetime²⁴ may synchronize for a narrower range of parameters if they exhibit very different LEF and this could complicate the enciphering process. The chaotic bubble can also be expanded for some values of the LEF and varying the value of the latter through temperature or current control can help to achieve complex chaotic behaviors, which are also of paramount importance in the case of secure communications. Indeed, the more complex is the chaotic pattern used to hide the message, the more difficult is the deciphering for a third party. The non-linear dynamics of laser diodes under external optical feedback can be studied through the Lang and Kobayashi model,²⁵ composed of two dimensionless equations :

$$\frac{dY}{ds} = (1 + i\alpha)ZY + \eta e^{(-i\Omega_0\theta)}Y(S - \theta), \quad (1)$$

$$T\frac{dZ}{ds} = P - Z - (1 + 2Z)|Y|^2, \quad (2)$$

With s the normalized time with respect to the photon lifetime τ_p , Y the normalized complex electric field and Z the normalized carrier density. α stands for the LEF. θ is the normalized external cavity roundtrip time, Ω_0 is the normalized laser frequency above threshold and P is defined as the normalized pump parameter, equal to :

$$P = \frac{\tau_p\tau_c G_N}{2q}(I - I_{th}), \quad (3)$$

Where G_N is the differential gain, τ_c the carrier lifetime and q the electron charge.

In Equation (1), η is the normalized feedback coefficient and scales as :

$$\eta = \frac{\tau_p}{\tau_{in}} 2C_l \sqrt{f}, \quad (4)$$

Where C_l is the coupling strength coefficient of the front facet that is coupled to the external cavity²⁶ and τ_{in} the photon roundtrip time in the laser cavity.

We use this model for a numerical analysis of the bifurcation diagrams when varying the value of the LEF. This model has initially been designed for diode lasers but the conventional set of rate equations for QCLs can be approximated with good accuracy by the aforementioned model.²⁷ The parameters are set as described in Table 1 and are very close to the experimental parameters, so the simulations can be appropriately compared with the experimental results below. Figure 2 (a)-(c) show the bifurcation diagram for this set of parameters

Parameter	value
Laser length, l	2 mm
Reflectivity of the output facet, R_1	0.3
Reflectivity of the back facet, R_2	0.95
Internal cavity refractive index, n	3.2
Normalized cavity roundtrip time, θ	500
Coupling strength coefficient, C_l	0.64
Photon lifetime, τ_p	4.7 ps
Carrier lifetime, τ_c	4.7 ps
Carrier-to-photon lifetime, T	1
Differential gain, G_N	$3.6 \times 10^5 \text{ s}^{-1}$
Normalized pump parameter, P	4
Current pumping difference, $(I - I_{th})$	160 mA

Table 1: Physical and structural parameters used in the calculations.

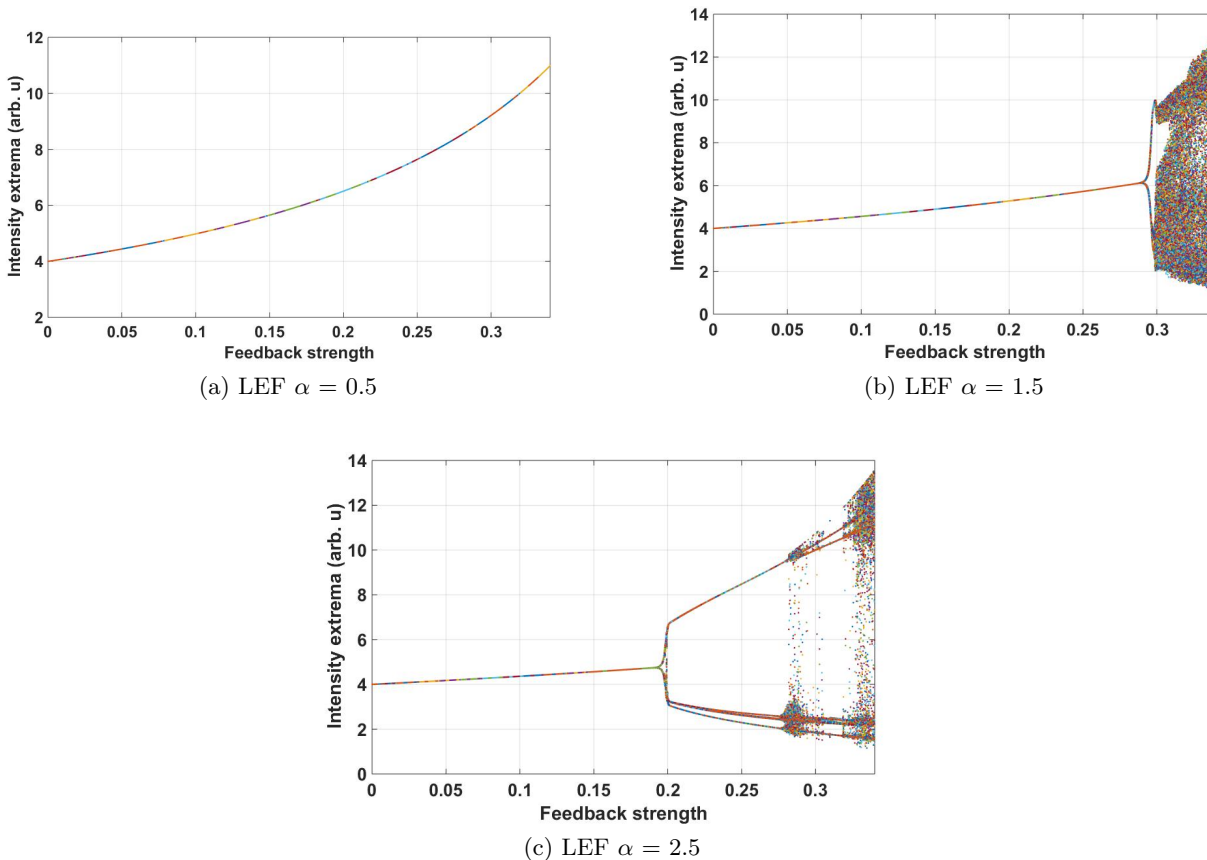


Figure 2: Bifurcation diagram for the parameters included in Table 1.

and a LEF of 0.5, 1.5 and 2.5, respectively. Bifurcation diagrams gather the output extrema with respect to the feedback strength (F) and allow analyzing the dynamics of the laser's output.

When the LEF equals 0.5 (Fig. 2 (a)), the output of the laser remains constant even for a feedback strength as high as 35%. Consequently, no dynamics are observed in this configuration which corresponds to values of LEF commonly found in QCLs.^{19,28} However, the lack of bifurcation is not compatible with experimental studies where the QCL is under conventional optical feedback.^{10,11} Figure 2 (b) shows the bifurcation diagram when the LEF is 1.5 and the other parameters remain constant. The output of the laser is constant until the feedback strength reaches 29%. Then, the Hopf bifurcation appears, meaning that the output enters an oscillatory state and eventually, the chaotic bubble is reached for a feedback strength of 30%. This bubble corresponds to the dense area in the diagram and means that the output exhibits several maxima and minima and this is related to a chaotic behavior. If the value of the LEF is increased to 2.5, the bifurcation diagram also displays a Hopf bifurcation, as shown in Fig. 2 (c), but for a lower feedback strength (19%). Then, the chaotic behavior is slightly different because not only one large chaotic bubble appears, like in the $\alpha = 1.5$ case, but several thin areas are retrieved. Each of them are separated by oscillatory states where the bifurcation diagram is composed of branches. The thin chaotic bubbles can for instance be found around $F = 20\%$, $F = 28\%$ and $F = 33\%$.

A comparison between the simulations and the results shown in experimental works^{10,11} tends to confirm a LEF value high above zero since experimentally, the destabilization occurs for feedback ratios in the order of 1%. This is counterintuitive in a sense that the reciprocal space curvature of the subbands in a QCL should give a LEF very close to zero.²⁹

4. EXPERIMENTS

4.1 Above-threshold measurements

The self-mixing interferometry method is a well known technique to obtain the LEF in the case of single-mode semiconductor lasers and has been successfully adapted for DFB-QCLs in the past.^{5,11} The method is based on the dependence of the intracavity mixing signal on the phase difference ϕ between the emitted and the back-reflected light. The so-called feedback phase ϕ can be, for example, varied by modulating the external cavity. An interferogram, the so-called selfmixing signal $P(\phi)$ is then obtained as a function of ϕ . Consequently, the optical output power of the laser is given by :

$$P(\phi) = P_0 (1 + mF(\phi)), \quad (5)$$

where P_0 represents the laser power without feedback and m is a modulation index. The interferometric function $F(\phi)$ depends on the LEF α and the feedback parameter C given by :

$$C = \epsilon_{\text{mm}} \frac{L\sqrt{1+\alpha^2}}{l \cdot n} \sqrt{R_{\text{ext}}} \cdot \frac{1-R_1}{\sqrt{R_1}}, \quad (6)$$

where ϵ_{mm} represents the mode mismatch parameter, L the length of the external cavity and l the length of the internal cavity. The variable n is the internal cavity refractive index, while R_{ext} represents the reflectivity of the feedback mirror and R_1 the reflectivity of the output facet.

The experimental setup to gather the selfmixing signal is shown in Fig. 3. The QCL's beam is split with a non-polarizing beam splitter and one part is being detected with a MCT-detector. The other part passes the beam splitter and is fed-back to the laser via a mirror, which is mounted on a linear piezo translation stage. A neutral-density filter (NDF) in the feedback arm allows controlling the feedback strength and remaining in the weak feedback regime. The translation stage is driven with a sine modulation of a 137 Hz.

In the case of weak feedback¹⁷ $0 < C < 1$, the expression

$$\alpha = \frac{T_M - 0.5}{T_C - 0.5} \quad (7)$$

holds,⁵ where T_M and T_C are time intervals, which are defined as

$$T_M \equiv \frac{T_{\text{max}} - T_{\text{min}}}{T} \quad (8)$$

$$T_C \equiv \frac{T_{C2} - T_{C1}}{T}. \quad (9)$$

The time-points T_{C2} and T_{C1} represent the positions of the consecutive zeros, T_{max} and T_{min} the positions of the consecutive extrema and the interval T is the period of the interferogram.

In Fig. 4 a), a cutout of the normalized waveform $P_{\text{norm}}(t) = (P(t) - P_0)/P_{\text{max}}$ for an injection current of $I_0 = 560$ mA is visualized, where $P_{\text{max}} = \max(P(t) - P_0)$. In that cutout the mirror moves linearly towards the laser, thus decreasing the feedback phase ϕ linearly. By determining the required time intervals T_M , T_C and T , which are highlighted in dark green, together with using Eq. 7 - 9, it is possible to obtain the LEF. The result in the case of an injection current of 560 mA amounts to 2.67 ± 0.45 . We do not show LEFs for currents lower than 560 mA, because the self-mixing signal was too noisy in this region resulting in a very high uncertainty of

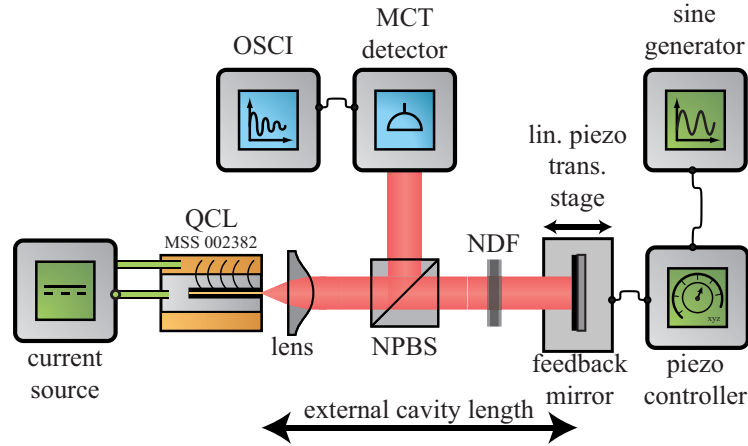


Figure 3: Schematic of setup to measure the LEF with oscilloscope (OSCI), MCT detector (Kolmar KMPV50 0.5 J2), non-polarizing beam splitter (NPBS) with 90:10 transmission/reflection ratio, current source (self-made battery), linear piezo translation stage, piezo controller and connected sine generator, lens as well as a neutral density filter (NDF) to control the feedback strength.

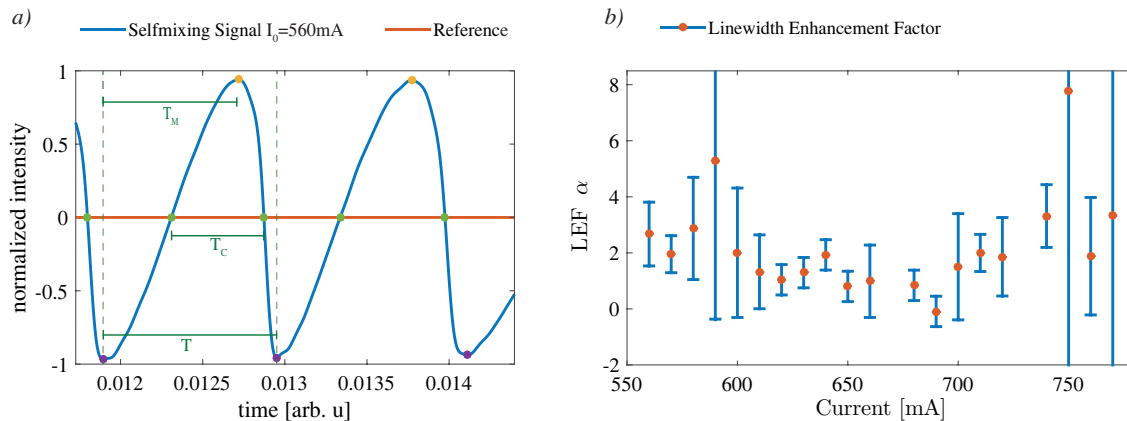


Figure 4: a) Cutout of the experimentally obtained normalized waveform from the weak feedback selfmixing signal of the QCL driven with an injection current of $I_0 = 560\text{mA}$ at the MCT-detector with the time intervals required for the determination of the LEF. The resulting LEF amounts to $\alpha = 2.67 \pm 0.45$. b) LEF as a function of the injection current.

the LEF value. Figure 4 b) depicts the influence of the injection current on the LEF. For that purpose, 100 waveforms were acquired at each injection current in order to derive the LEF. The orange dots represent the mean value of the determined LEFs and the blue error-bars depict the standard-deviation of all determinations. It can be seen that for all injection currents, the LEF value remains positive. For low injection currents the LEF is around 2, while it becomes close to 0 for injection currents between 650 mA and 700 mA. For higher injection currents the LEF increases to values around 4. Such large values could be explained by the pumping far above threshold but could also result from the DFB grating which alters the structure of the initial Fabry-Perot laser. This modification can be responsible for spatial non-linearities such as spatial hole burning (SHB) and have an influence on the LEF of the QCL.³⁰ These values high above zero are compatible with the chaotic patterns we were able to retrieve with mid-infrared quantum cascade lasers, as aforementioned in the section about the numerical analysis. Indeed, if the LEF is too close to zero, the non-linear dynamics cannot be exhibited, even for large feedback strengths, as already pointed out.²⁷

4.2 Below-threshold measurements

When pumped below threshold, the QCL only emits very few output power due to the spontaneous emission. Thus, the self-mixing interferometry technique cannot be applied to retrieve the LEF in this range of pumping current. Moreover, as the laser is powered below threshold, it does not emit single mode anymore and the optical spectrum is that of a Fabry-Perot laser. This allows using the Hakki-Paoli method, also called Amplified Spontaneous Emission (ASE) method,¹³ to retrieve the LEF. The aforementioned setup is no longer useful in this section and the output of the QCL is directly analyzed with a Fourier transform infrared (FTIR) spectrometer (Bruker Vertex 80V). Figure 5 a) shows the Fabry-Perot spectra retrieved from 255 mA to 325 mA. 255 mA is the minimum current value for which a signal can be detected and 325 mA corresponds to the current value just below threshold. The ASE method relies on the evolution of the Fabry-Perot spectra when varying the pump current, and more precisely the shifting of the modes. Figure 5 b) shows a close-up on the modes we will focus on to derive the LEF below threshold. The modal gain G , expressed for a pumping current, is given by³¹ :

$$G = \frac{1}{l} \ln\left(\frac{\sqrt{\Delta I} - 1}{\sqrt{\Delta I} + 1}\right) + \frac{1}{2l} \ln\left(\frac{1}{R_1 R_2}\right), \quad (10)$$

With l the length of the laser's cavity, $\Delta I = I_{max}/I_{min}$ the ratio of the maximum and the minimum of the Fabry-Perot spectrum and R_1 and R_2 the reflectivities of the laser's facets. The change in refractive index Δn is then obtained from the peak wavelength shift $\Delta \lambda$ when increasing the pumping current³¹ :

$$\Delta n = \frac{\lambda}{2l} \times \frac{\Delta \lambda}{\lambda_{FP}}, \quad (11)$$

With λ_{FP} the mode spacing in the Fabry-Perot spectrum. When increasing the pumping current, the change in the modal gain and the variation of the refractive index are used to extract the LEF³² :

$$\alpha = -\frac{4\pi}{\lambda} \times \frac{\Delta n}{\Delta G}, \quad (12)$$

For the calculation of the LEF, we focus on the optical spectra at 290 mA and 305 mA, whose maxima are marked with green circles and purple circles in Fig. 5 b), respectively. The experimental data selected for the derivation are those around 5390 nm because the modal gain is more homogeneous in this spectral window (see Fig. 5 a)) than close to the maximum output of the laser, which is fixed at 5450 nm by the DFB grating. The extracted gain spectra are represented in Fig. 6 a) for various pumping current conditions. Since the measurement is done under continuous-wave conditions, the wavelength red-shift caused by thermal effects must be fully eliminated so that we only account for the net carrier induced effects.³³ In such purpose, the wavelength shift below threshold is estimated from the wavelength red-shift due to thermal effects above threshold, the latter being $0.49 \text{ \AA} \cdot \text{mA}^{-1}$ between 360 mA and 500 mA. The spectral dependence of the LEF is plotted in Fig. 6 b). The retrieved LEF is around -0.4 and differs from the value found with the self-mixing interferometry technique above threshold. The latter is however retrieved for current values high above threshold and cannot be compared with values found close to and below threshold. Furthermore, numerical simulations have already demonstrated a LEF increasing from negative values to positive values in the case of QCLs.³⁴

5. CONCLUSIONS

We have combined two experimental techniques in order to retrieve the LEF of a QCL emitting at $5.45 \mu\text{m}$. The value below threshold is close to -0.4 and above threshold, the value fluctuates between 0 and 4 with most of the values included in the range $\alpha = 2 \pm 1$. This experimental study is complemented by a numerical analysis confirming that the non-linear dynamics observed in QCLs with external optical feedback require a LEF greater than 1.5, which is compatible with the LEF values found above threshold. This result differs from prior theoretical and experimental studies focusing on intersubband transitions since this configuration should produce a LEF equal to zero. Therefore, further investigation will determine the LEF under high-frequency modulation

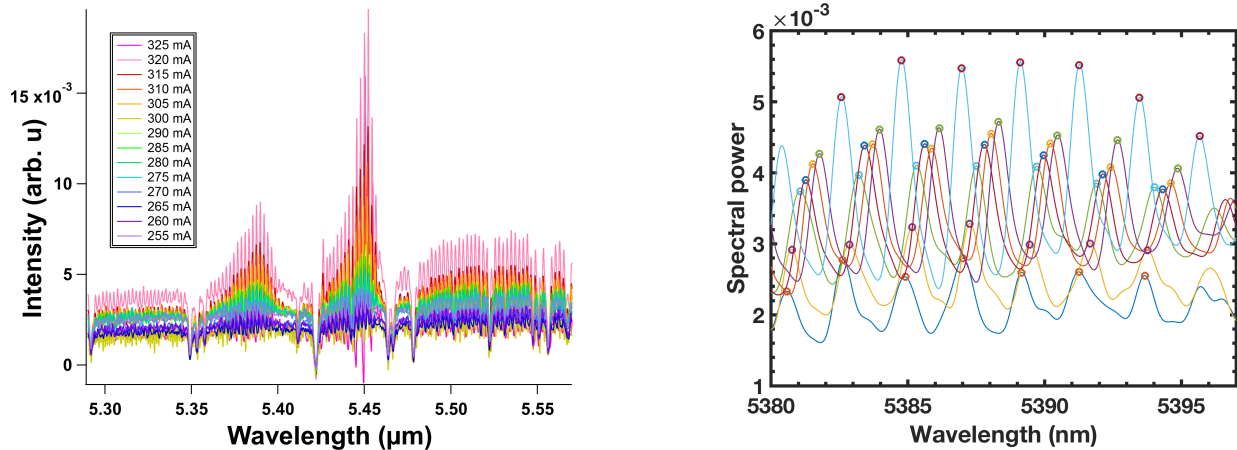


Figure 5: Experimental optical spectra below threshold for a pumping current varying from 255 mA to 325 mA in steps of 5 mA (a) and close-up around $5.39 \mu\text{m}$ (b) for pumping currents shown in Fig. 6 a).

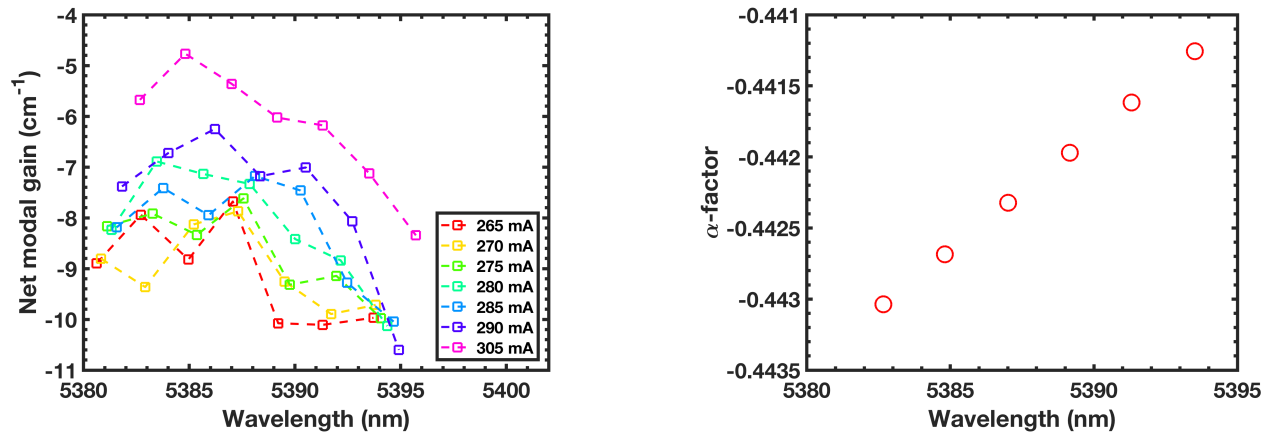


Figure 6: Net modal gain with respect to the wavelength for several pumping current below threshold (a) and calculated LEF when comparing the data at 290 mA and 305 mA (b).

in order to confirm the tendency we observed. Such method^{29,35} allows a global removal of the thermal effects that may still be present at a few dozens of MHz, corresponding to the characteristic frequencies of the chaotic patterns we observed.

Acknowledgments

This work is supported by the French Defense Agency (DGA) and the French ANR program under grant ANR-17-ASMA-0006. The authors thank Dr. Lukas Drzewietzki for the device interfaces for the experimental data acquisition.

REFERENCES

- [1] Yao, Y., Hoffman, A. J., and Gmachl, C. F., "Mid-infrared quantum cascade lasers," *Nature Photonics* **6**(7), 432 (2012).
- [2] Capasso, F., "High-performance midinfrared quantum cascade lasers," *Optical Engineering* **49**(11), 111102 (2010).
- [3] Henry, C., "Theory of the linewidth of semiconductor lasers," *IEEE Journal of Quantum Electronics* **18**(2), 259–264 (1982).

- [4] Jumpertz, L., Michel, F., Pawlus, R., Elsässer, W., Schires, K., Carras, M., and Grillot, F., “Measurements of the linewidth enhancement factor of mid-infrared quantum cascade lasers by different optical feedback techniques,” *AIP Advances* **6**(1), 015212 (2016).
- [5] Von Staden, J., Gensty, T., Elsässer, W., Giuliani, G., and Mann, C., “Measurements of the α factor of a distributed-feedback quantum cascade laser by an optical feedback self-mixing technique,” *Optics Letters* **31**(17), 2574–2576 (2006).
- [6] Hakki, B. W. and Paoli, T. L., “Gain spectra in gas double-heterostructure injection lasers,” *Journal of Applied Physics* **46**(3), 1299–1306 (1975).
- [7] Jumpertz, L., [*Nonlinear Photonics in Mid-infrared Quantum Cascade Lasers*], Springer (2017).
- [8] Jumpertz, L., Carras, M., Schires, K., and Grillot, F., “Regimes of external optical feedback in 5.6 μm distributed feedback mid-infrared quantum cascade lasers,” *Applied Physics Letters* **105**(13), 131112 (2014).
- [9] Tkach, R. and Chraplyvy, A., “Regimes of feedback effects in 1.5 μm distributed feedback lasers,” *Journal of Lightwave Technology* **4**(11), 1655–1661 (1986).
- [10] Spitz, O., Wu, J., Carras, M., Wong, C.-W., and Grillot, F., “Low-frequency fluctuations of a mid-infrared quantum cascade laser operating at cryogenic temperatures,” *Laser Physics Letters* **15**(11), 116201 (2018).
- [11] Jumpertz, L., Schires, K., Carras, M., Sciamanna, M., and Grillot, F., “Chaotic light at mid-infrared wavelength,” *Light: Science & Applications* **5**(6), e16088 (2016).
- [12] Osinski, M. and Buus, J., “Linewidth broadening factor in semiconductor lasers—an overview,” *IEEE Journal of Quantum Electronics* **23**(1), 9–29 (1987).
- [13] Henning, I. and Collins, J., “Measurement of the linewidth broadening factor of semiconductor lasers,” *Electron. Lett* **19**, 927–929 (1987).
- [14] Kikuchi, K. and Okoshi, T., “Estimation of linewidth enhancement factor of AlGaAs lasers by correlation measurement between FM and AM noises,” *IEEE Journal of Quantum Electronics* **21**(6), 669–673 (1985).
- [15] Liu, G., Jin, X., and Chuang, S., “Measurement of linewidth enhancement factor of semiconductor lasers using an injection-locking technique,” *IEEE Photonics Technology Letters* **13**(5), 430–432 (2001).
- [16] Yu, Y., Giuliani, G., and Donati, S., “Measurement of the linewidth enhancement factor of semiconductor lasers based on the optical feedback self-mixing effect,” *IEEE Photonics Technology Letters* **16**(4), 990–992 (2004).
- [17] von Staden, J., Gensty, T., Peil, M., Elsässer, W., Giuliani, G., and Mann, C., “Measurement of the linewidth enhancement factor of quantum cascade lasers by the self-mixing technique,” in [*Semiconductor Lasers and Laser Dynamics II*], **6184**, 61841E, International Society for Optics and Photonics (2006).
- [18] Green, R. P., Xu, J.-H., Mahler, L., Tredicucci, A., Beltram, F., Giuliani, G., Beere, H. E., and Ritchie, D. A., “Linewidth enhancement factor of terahertz quantum cascade lasers,” *Applied Physics Letters* **92**(7), 071106 (2008).
- [19] Hangauer, A. and Wysocki, G., “Gain compression and linewidth enhancement factor in mid-IR quantum cascade lasers,” *IEEE J. Sel. Top. Quantum Electron* **21**(6), 1200411 (2015).
- [20] Cardilli, M. C., Dabbicco, M., Mezzapesa, F. P., and Scamarcio, G., “Linewidth measurement of mid infrared quantum cascade laser by optical feedback interferometry,” *Applied Physics Letters* **108**(3), 031105 (2016).
- [21] Blaser, S., Hofstetter, D., Beck, M., and Faist, J., “Free-space optical data link using Peltier-cooled quantum cascade laser,” *Electronics Letters* **37**(12), 778–780 (2001).
- [22] Sciamanna, M. and Shore, K. A., “Physics and applications of laser diode chaos,” *Nature Photonics* **9**(3), 151 (2015).
- [23] Murakami, A. and Ohtsubo, J., “Synchronization of feedback-induced chaos in semiconductor lasers by optical injection,” *Physical Review A* **65**(3), 033826 (2002).
- [24] Mirasso, C. R., “Applications of semiconductor lasers to secure communications,” in [*AIP Conference Proceedings*], **548**(1), 112–127, AIP (2000).
- [25] Lang, R. and Kobayashi, K., “External optical feedback effects on semiconductor injection laser properties,” *IEEE journal of Quantum Electronics* **16**(3), 347–355 (1980).
- [26] Grillot, F., “On the effects of an antireflection coating impairment on the sensitivity to optical feedback of AR/HR semiconductor DFB lasers,” *IEEE Journal of Quantum Electronics* **45**(6), 720–729 (2009).

- [27] Erneux, T., Kovanis, V., and Gavrielides, A., “Nonlinear dynamics of an injected quantum cascade laser,” *Physical Review E* **88**(3), 032907 (2013).
- [28] Liu, T., Lee, K. E., and Wang, Q. J., “Importance of the microscopic effects on the linewidth enhancement factor of quantum cascade lasers,” *Optics Express* **21**(23), 27804–27815 (2013).
- [29] Aellen, T., Maulini, R., Terazzi, R., Hoyler, N., Giovannini, M., Faist, J., Blaser, S., and Hvozdar, L., “Direct measurement of the linewidth enhancement factor by optical heterodyning of an amplitude-modulated quantum cascade laser,” *Applied physics letters* **89**(9), 091121 (2006).
- [30] Aoki, M., Uomi, K., Tsuchiya, T., Sasaki, S., and Chinone, N., “Stabilization of the longitudinal mode against spatial hole burning in $\lambda/4$ -shifted DFB lasers by quantum size effect,” *IEEE photonics technology letters* **2**(9), 617–619 (1990).
- [31] Minch, J., Chuang, S.-L., Chang, C.-S., Fang, W., Chen, Y.-K., and Tanbun-Ek, T., “Theory and experiment on the amplified spontaneous emission from distributed-feedback lasers,” *IEEE Journal of Quantum Electronics* **33**(5), 815–823 (1997).
- [32] Lerttamrab, M., Chuang, S.-L., Gmachl, C., Sivco, D., Capasso, F., and Cho, A., “Linewidth enhancement factor of a type-i quantum-cascade laser,” *Journal of applied physics* **94**(8), 5426–5428 (2003).
- [33] Wang, C., Schires, K., Osiński, M., Poole, P. J., and Grillot, F., “Thermally insensitive determination of the linewidth broadening factor in nanostructured semiconductor lasers using optical injection locking,” *Scientific reports* **6**, 27825 (2016).
- [34] Pereira, M., “The linewidth enhancement factor of intersubband lasers: From a two-level limit to gain without inversion conditions,” *Applied Physics Letters* **109**(22), 222102 (2016).
- [35] Hangauer, A., Spinner, G., Nikodem, M., and Wysocki, G., “High frequency modulation capabilities and quasi single-sideband emission from a quantum cascade laser,” *Optics express* **22**(19), 23439–23455 (2014).